

Special Issue “Materiais 2015”

## Influence of heat treatments on the sensitization of a supermartensitic stainless steel

S.S.M. Tavares<sup>a,\*</sup>, M.R. Silva<sup>b</sup>, J.M. Pardal<sup>a</sup>, M.B. Silva<sup>c</sup>, M.C.S. de Macedo<sup>c</sup>

<sup>a</sup>Universidade Federal Fluminense, Rua Passo da Pátria, 156 – CEP 24210-240, Niterói, Brazil

<sup>b</sup>Universidade Federal de Itajubá, Instituto de Ciências, Itajubá/MG, Brazil

<sup>c</sup>Universidade Federal do Espírito Santo, Departamento de Engenharia Mecânica, Vitória/ES, Brazil

### Abstract

Supermartensitic stainless steels with 12-13% Cr show higher corrosion resistance than conventional grades such as UNS S42000 and S41000. The reduction of carbon content to less than 0.03%, and the addition of Ni and Mo are the most important compositional changes which enhances mechanical properties and corrosion resistance. Ti addition is used to combine with C and N, and avoid Cr carbides precipitation and to improve mechanical properties. In general, SMSS steels are quenched and tempered or double tempered. The purpose of this work was to investigate how the microstructure and the corrosion decay by sensitization are influenced by quenching and tempering heat treatments in a novel supermartensitic 13% Cr stainless steel with Ti addition. DL-EPR (double loop potentiokinetic electrochemical reactivation) test was used to obtain the degree of sensitization (DOS). The results show that, despite the extra low carbon content, and the stabilization with Ti, the material can become sensitized with heat treatments. The sensitization is rather related to Ti(C, N) precipitation and reverse austenite than to Cr carbides.

© 2017 Portuguese Society of Materials (SPM). Published by Elsevier España, S.L.U. All rights reserved.

**Keywords:** Supermartensitic steels; microstructure; intergranular corrosion; sensitization.

### 1. Introduction

Supermartensitic stainless steels (SMSS) with 12-13% Cr show higher corrosion resistance than conventional grades such as UNS S42000 and S41000. The reduction of carbon content to less than 0.03%, and the addition of Ni and Mo are the most important compositional changes which enhances mechanical properties and corrosion resistance [1].

Sensitization can be defined as intergranular chromium carbide precipitation which causes Cr depletion in the vicinity of grain boundaries. As a consequence, the steel becomes susceptible to intergranular corrosion when exposed to aggressive environments. These Cr-depleted regions present a weakest passive layer, with an anodic behaviour in

front of the unaffected zones [2-5]. In fact, sensitization may not be restricted to chromium carbides precipitation but also includes other Cr rich phases [6-8]. Besides, although intergranular precipitation is more common, intragranular precipitates may also cause chromium depletion and localized corrosion.

Supermartensitic steels must be quenched and tempered, or double tempered, to achieve optimum mechanical properties. The heat treatments also change the corrosion resistance of the steel. Different types of corrosion, such as pitting, intergranular and stress corrosion cracking are connected and closely related to microstructural features. In particular, precipitation reactions may provoke sensitization and corrosion decay. Although SMSSs are less susceptible than conventional stainless steels, some works have shown that these extra low carbon materials can also become sensitized [5,9-12]. Nakamichi *et al.* [5] studied the intergranular corrosion cracking in the heat affected zone (HAZ) of a 11% Cr SMSS, and found

\* Corresponding author.

E-mail address: [ssmtavares@terra.com.br](mailto:ssmtavares@terra.com.br) (Sérgio S.M. Tavares)

that the extension of the Cr depleted zone was about 10 to 15 nm. Ladanova *et al.* [9] also measured the width of the Cr-depleted zone and found about 25 nm around  $M_{23}C_6$  carbides in the as welded HAZ. After post weld heat treatment (PWHT) at 640°C the Cr depletion was eliminated due to the diffusion (healing). Aquino *et al.* [10] and Della Rovere *et al.* [11] studied the sensitization of weld joints of SMSS using double loop electrochemical potentiodynamic reactivation tests (DL-EPR). In a previous work of our group this technique was also used to analyse a Ti-alloyed SMSS [12].

The addition of Ti and/or Nb is supposed to increase the intergranular corrosion resistance of SMSS, as already observed in austenitic [13] and ferritic stainless steels [14,15]. However, even stabilized steels may undergo sensitization, as observed in previous works [11,12,16].

The purpose of this work was to investigate how the microstructure and the degree of sensitization of a novel SMSS 12% Cr stainless steel with Ti addition are influenced by quenching and tempering. In a previous work, the effect of tempering treatments after quenching from 1000°C was investigated [12]. In this work, double and triple quenching treatments were tested in order to produce new and finer microstructures. After quenching treatments, single and double tempering treatments were performed.

## 2. Materials and Methods

The material used in the study was obtained from a seamless tube of Ti alloyed 13% Cr SMSS with chemical composition shown in Table 1.

Table 1. Chemical composition of supermartensitic stainless steel studied (wt.%).

C	Cr	Ni	Mo	Mn	Ti	P	S	N
0.028	12.21	5.8	1.95	0.52	0.28	0.011	0.001	0.01

The temperatures  $M_s$  (martensite start),  $M_f$  (martensite final),  $A_1$  and  $A_3$  were determined by dilatometry using cylindrical specimens with 6.00 mm diameter and 10.00 mm length. The heating rate applied was 5°C/min.

The specimens were cut and machined with 15x15x10 mm dimensions for double loop electrochemical potentiodynamic (DL-EPR) tests. Before the confection of working electrodes for DL-EPR, the specimens were heat treated.

Three quenching treatments were performed, as shown in Fig. 1. Q1 is a single water quenching with soaking at 1000°C for 1 h. Q2 is a double quenching treatment,

with the same cycle of Q1, followed by a second soaking at 900°C for 1h and water quenching. Q3 is a triple quenching treatment, with the same cycles of Q2, followed by a third quenching with soaking at 800°C. After quenching, some specimens were single or double tempered according to Table 2.

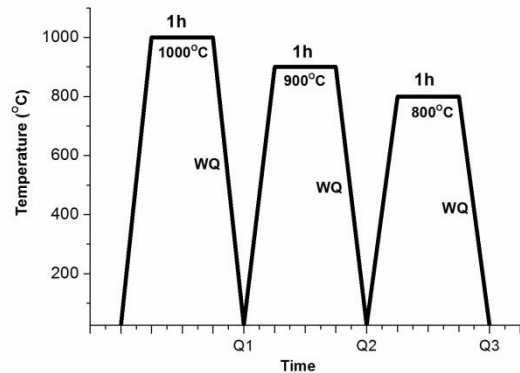


Fig. 1. The quenching treatments performed.

The DL-EPR tests were carried out in a conventional three cell electrode assembled with working electrode, Pt foil as auxiliary electrode, and saturated calomel electrode (SCE) as reference. The working electrode was constructed using the supermartensitic specimens embedded in epoxy resin with a copper wire for electric contact. Usually, the working electrodes were ground with 400 emery paper and cleaned in water. However, some electrodes were polished with diamond paste in order to observe the surface after test in the scanning electron microscope (SEM). The tests were controlled by a potentiostat-galvanostat. The test solution was composed of 0.25 mol/L  $H_2SO_4$  + 0.01 mol/L KSCN. Before the test, the open circuit potential ( $E_{OCP}$ ) was stabilized for 30 min. The potential was then increased in the anodic direction at 1 mV/s up 0.3  $V_{SCE}$ . Then, the scan was reversed, using the same sweeping rate in the cathodic direction. The parameters extracted from the DL-EPR were the  $Ir/Ia$  and  $Ar/Aa$  ratios, where  $Ir$  and  $Ia$  are the peak currents in the reactivation and activation peaks, and  $Ar$  and  $Aa$  are the areas of the reactivation and activation loops, respectively. According to the literature, these two parameters give a measure of the degree of sensitization (DOS) of the steel [17]. In this work the  $Ir/Ia$  and  $Ar/Aa$  were compared. The tests were done in triplicate, using three specimens per heat treatment condition. Average values are presented in the results.

Microstructural investigation was performed by optical and scanning electron microscopy (SEM). The microstructures were revealed by Villela's etching (95 mL ethanol, 5 mL HCl and 1 g picric acid). Some

samples were observed after the DL-EPR tests to observe the regions preferentially attacked in the microstructure. In this case, the DL-EPR promoted the etching of previously polished samples.

Austenite fractions were quantified by means of magnetic measurements in a Vibrating Sample Magnetometer, using small specimens extracted from the heat treated samples. This method is based on the magnetization saturation measurement, considering that austenite is paramagnetic and martensite is ferromagnetic. More details of this analysis can be found in references [12] and [18].

Table 2. Tempering treatments and specimens identification.

Quenching	Single tempering			Double tempering
	500°C/1h	600°C/1h	650°C/1h	670°C/2h + 600°C/2h
Q1	Q1-500	Q1-600	Q1-650	Q1-DT1
Q2	Q2-500	Q2-600	Q2-650	Q2-DT1
Q3	Q3-500	Q3-600	Q3-650	Q3-DT1

### 3. Results and Discussion

#### 3.1. Quenched specimens Q1, Q2 and Q3

Fig. 2 shows the curve of dilatometry used to determine the  $A_{c1}$ ,  $A_{c3}$ ,  $M_s$  and  $M_f$  temperatures of the steel. Since the  $A_{c3}$  value measured was 722°C, the three soaking temperatures used in the triple quenching treatment (1000°C, 900°C and 800°C) are all in the austenitic field.

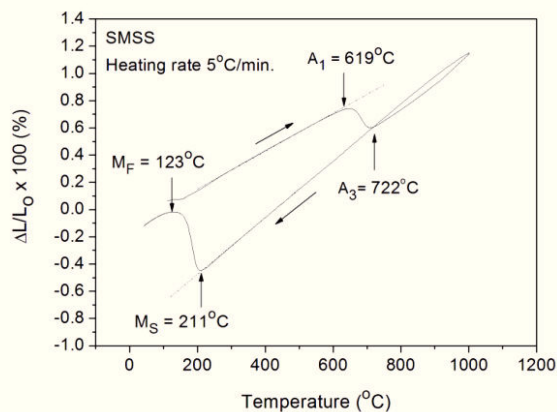


Fig. 2. Curve of dilatometric analysis of the studied supermartensitic steel.

Fig. 3 shows the typical DL-EPR curves of the specimens Q1, Q2 and Q3. The  $I_r/I_a$  and  $A_r/A_s$  values measured from these curves are presented in Table 3. It can be observed that the two parameters used to

measure the degree of sensitization (DOS) show the same behaviour.

The only condition that did not show any sign of sensitization was that of the specimen single quenched from 1000°C (Q1). The DOS increased with the second quenching from 900°C (specimen Q2), and further increased with the third quenching from 800°C (specimen Q3).

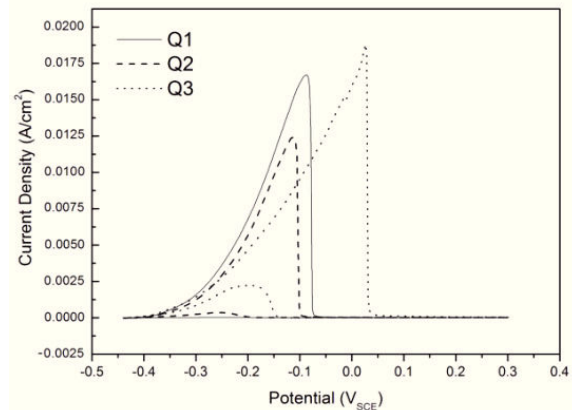


Fig. 3. DL-EPR curves of specimens Q1, Q2 and Q3.

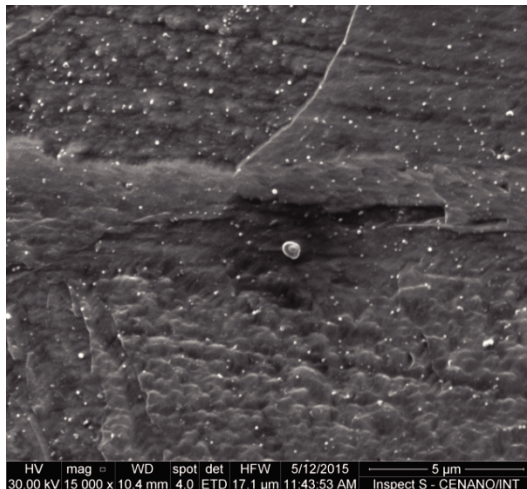
Figs. 4 (a-c) show the microstructures of Q1, Q2 and Q3. These three specimens have a martensitic matrix with fine and coarse precipitates. The coarse precipitates are square shaped TiN particles (not shown in Figs. 4 (a-c)). The fine precipitates which can be observed in Figs. 4 (a-c) are Ti rich particles, with shape and morphology similar to Ti(C, N) particles reported by Rodrigues *et al.* [19]. In a qualitative analysis, the density of these fine Ti-rich precipitates increases from Q1 to Q3, indicating that the increase of soaking temperature enhances the dissolution of these precipitates. On the other hand, the triple quenching treatment produces a higher amount of Ti(C, N) dispersed in a finer martensitic microstructure.

Figs. 5 a) and b) compare the microstructures of Q1 and Q3 with high magnification. The comparison of these images shows that the martensitic matrix of Q3 is finer and subdivided into cells or subgrains. Besides, as Fig. 5 b) is a composition of secondary electrons (SE) image with backscattered electron (BSE) image, it suggests that the matrix of Q3 has composition heterogeneities, probably due to the lower soaking temperature of the third quenching treatment (800°C).

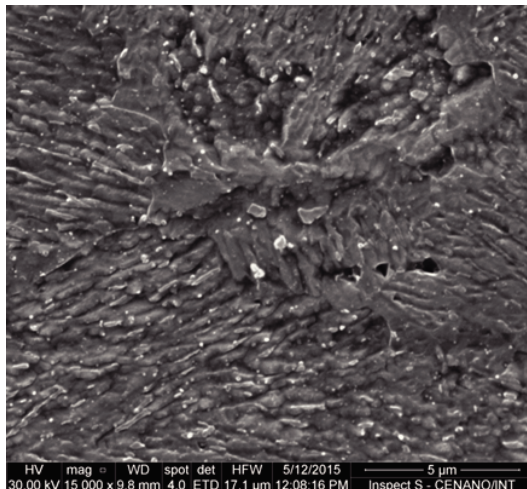
Figs. 6 (a-c) show the images of specimens Q1, Q2 and Q3 after the DL-EPR tests. It is clearly observed the increase of corrosion attack from Q1 to Q3, in accordance to the DOS results (Table 3). In these images the coarse TiN particles are shown.



a)

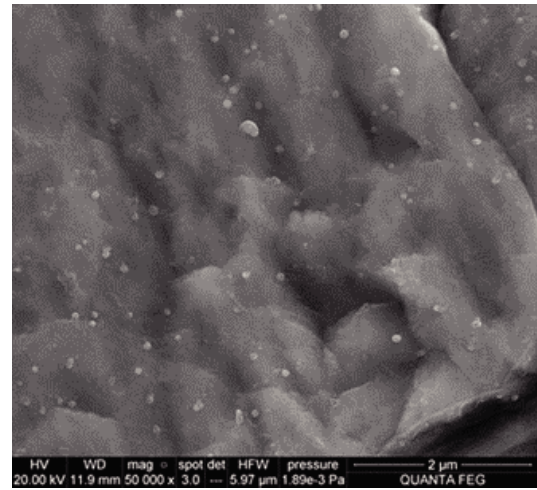


b)

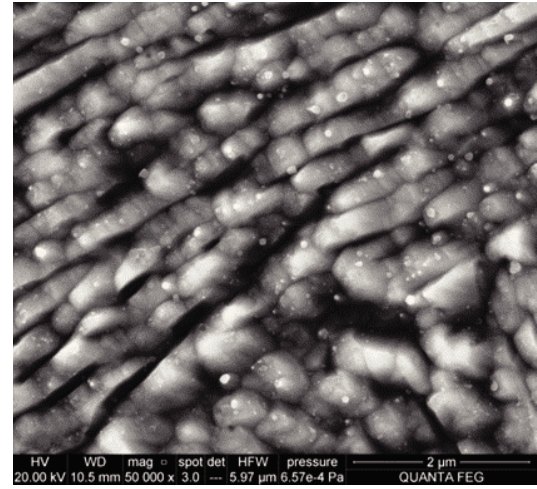


c)

Fig. 4. Microstructures of specimens quenched: Q1 (a), Q2 (b) and Q3 (c).



a)



b)

Fig. 5. Microstructures of specimens Q1 (a) and Q3 (b). SEM composition images BSE/SE.

The surface of specimen Q3 was severely damaged, showing many holes. These images also show that the sensitization of Q2 and Q3 is not restricted to grain boundaries regions.

The sensitization of specimens Q2 and Q3 cannot be explained by Cr carbides precipitation since the steel is over stabilized with Ti, and Cr carbides were not observed. Sensitization of stabilized stainless steels was studied by Kim *et al.* [14] which proposed that the corrosion attack is due to Cr segregation (not precipitation) in the vicinity of TiC particles, leaving a poor Cr zone. On the other hand, according to Ladanova *et al.* [9], TiC particles dissolves Cr and Mo and creates Cr-depleted areas around them.

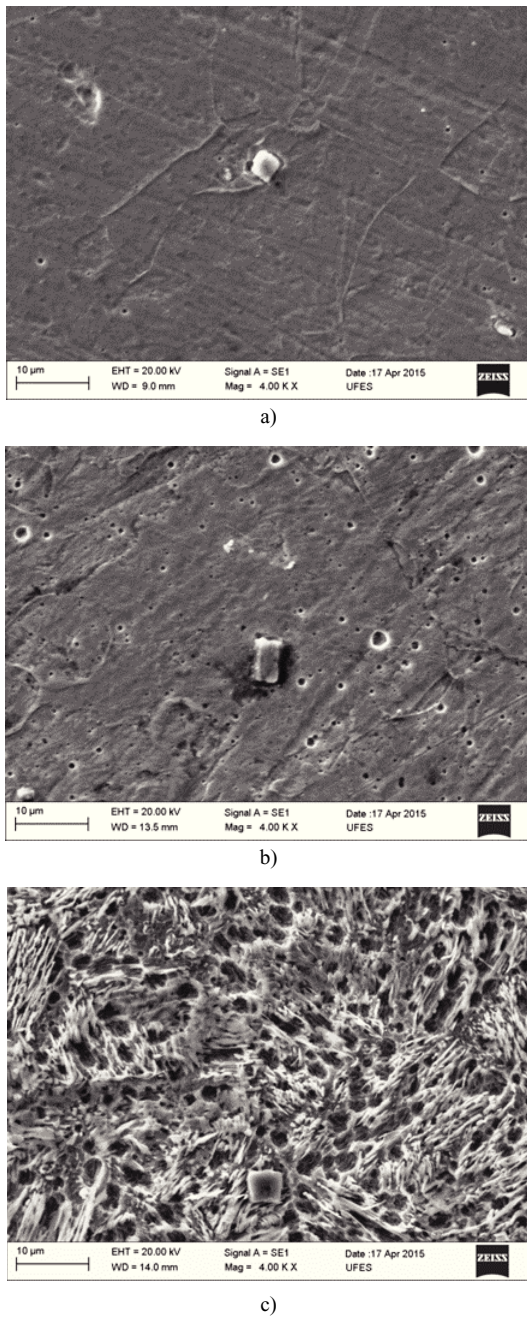


Fig. 6. Microstructures of quenched specimens after DL-EPR tests: Q1 (a), Q2 (b) and Q3 (c).

Table 3. Parameters Ir/Ia and Ar/Aa of specimens Q1, Q2 and Q3 (average of 3 tests).

Specimen	Ir/Ia	Ar/Aa
Q1	0.000	0.000
Q2	0.030	0.026
Q3	0.105	0.088

### 3.2. Quenched and tempered specimens Q1, Q2 and Q3

Figs. 7 a) and b) show the variation of the DOS (Ar/Aa and Ir/Ia) with the heat treatment. In specimens single tempered, the DOS parameters increased with the increase of tempering temperature, except for specimen triple quenched and tempered at 650°C (Q3-650).

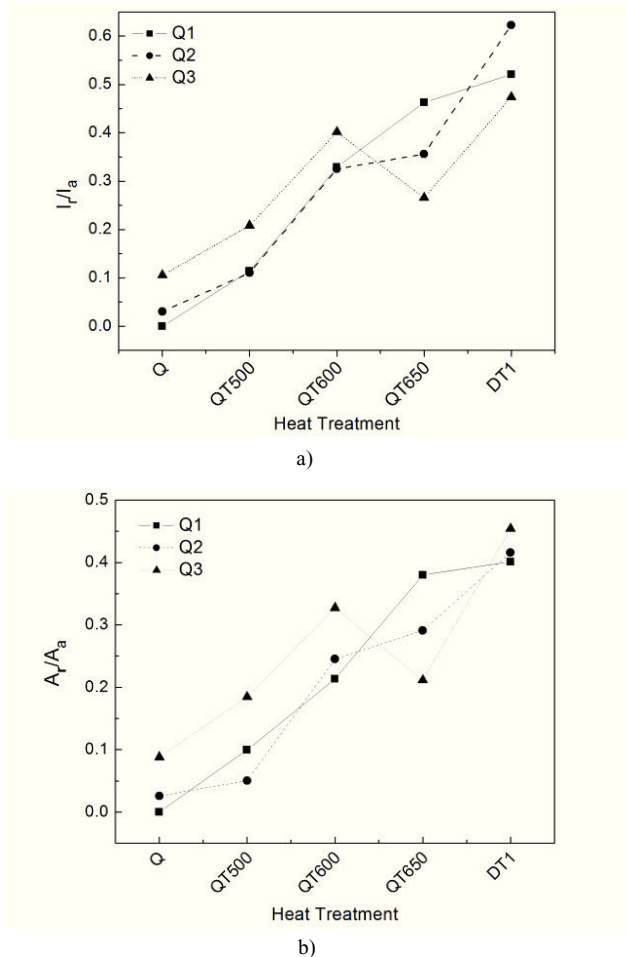


Fig. 7. DOS parameters as function of heat treatment: Ir/Ia (a), Ar/Aa (b).

In specimens tempered at 500°C, the corrosion attack was characterized by many holes, not restricted to grain boundaries, as shown in Fig. 8. It is also observed corrosion attack around the TiN particles, suggesting that these regions also became Cr depleted. The microstructures of specimens quenched and tempered at 650°C are characterized by tempered martensite and some reverse austenite, as observed in previous works [12].

Fig. 9 presents the variation of austenite content with heat treatments.

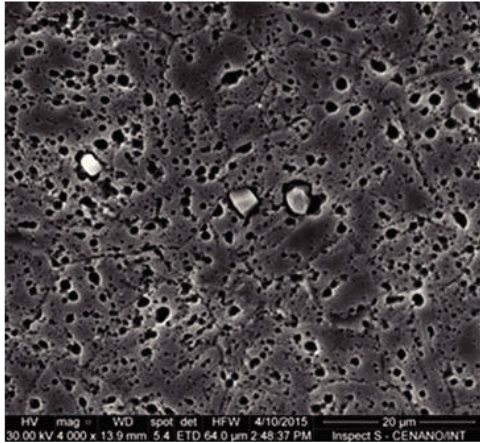


Fig. 8. Microstructure of specimen Q1-500 after DL-EPR test.

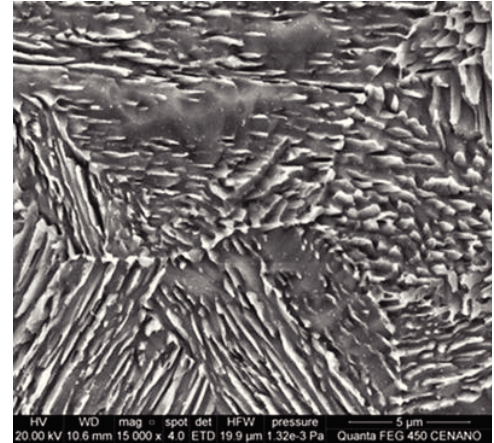


Fig. 10. Microstructure of Q1-650 revealed by Vilella's etching.

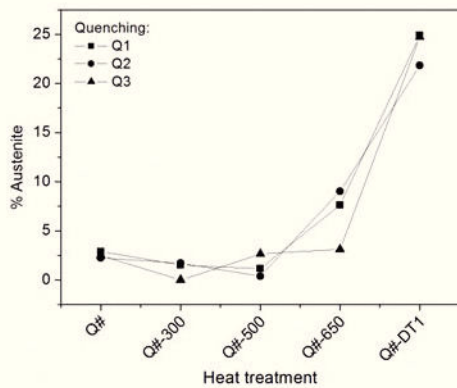
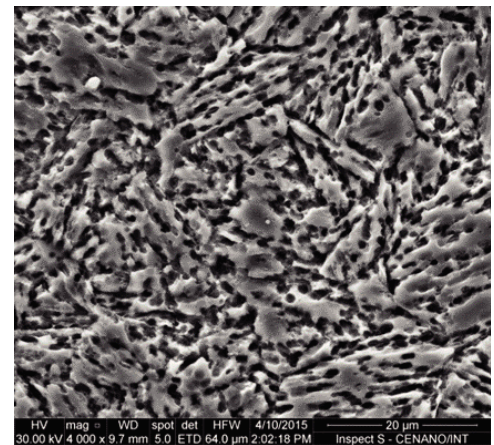
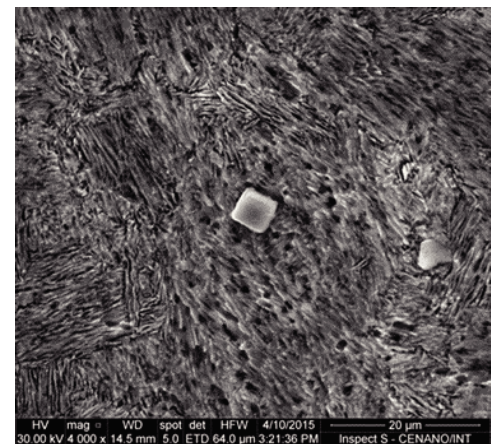


Fig. 9. Percentage of austenite as function of heat treatment.

Fig. 10 shows the microstructure of specimen Q1-650 revealed by Vilella's reagent. In this microstructure, the reverse austenite was formed in the prior austenite grain boundaries and between the martensite laths. The reverse austenite contains higher Ni and lower Cr and Mo than the matrix. Thus, as a consequence, the attack of specimen Q1-650 was characterized by localized corrosion of interlath reverse austenite, as shown in Fig. 11 a). The preferential dissolution of austenite in tempered SMSS was also observed by Della Rovere *et al.* [11]. On the other hand, according to the data of Fig. 9, the amount of austenite of specimen Q3-650 is considerably lower than that of Q1-650 and Q2-650, which can be explained by the higher amount of Ti(C, N) particles produced by the triple quenching treatment. A possible explanation for the lower DOS of specimen Q3-650, in comparison to Q2-650 and Q1-650, is related to the lower austenite content of Q3-650. This finding is corroborated by the observation of the surface of Q3-650 after DL-EPR test (Fig. 11 b)), in which the corrosion attack is much less pronounced than in specimen Q1-650.



a)

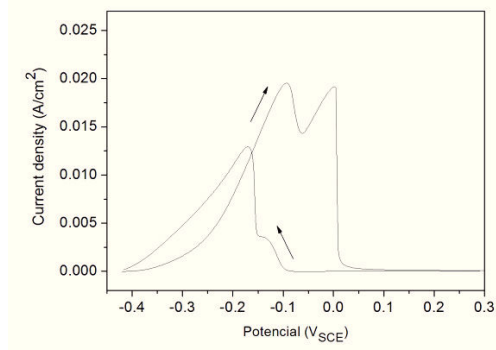


b)

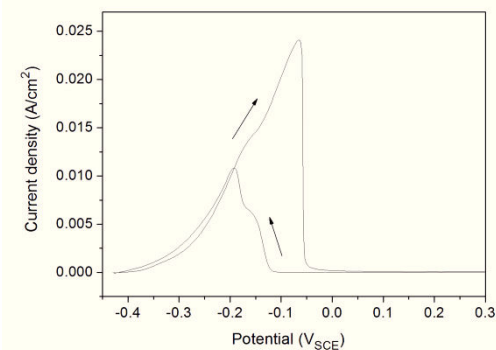
Fig. 11. Microstructures of specimens Q1-650 (a) and Q3-650 (b), after the DL-EPR tests.

The decrease of DOS from condition Q3-600 to Q3-650 (Figs. 7 a) and b)) indicates that a healing process lied to Cr diffusion is occurring in the triple quenched specimens.

Double tempered specimens have austenite contents between 21% and 23% (Fig. 9), and very high DOS parameters (Figs. 7 a) and b)). Also, the DL-EPR curves of all double quenched specimens (Q1-DT1, Q2-DT1 and Q3-DT1) exhibit clearly two activation peaks and two reactivation peaks, as shown in Fig. 12 a) (Q1-DT1). Two activation peaks were also observed by Della Rovere *et al.* [11] in a Ti alloyed SMSS with 12.2% of austenite. The first peak was attributed to the attack of martensite and the second peak to the dissolution of reversed austenite. Similar interpretation was done by Čihal and Štefec [17] for the split of the reactivation peak in a quenched and tempered low carbon Cr14Ni4Mo steel. The first peak was attributed to dissolution of the martensitic matrix, and the second peak, at a higher positive potential, was linked with the dissolution of a Ni rich phase, which may be the reverse austenite or a fresh martensite originated from this reverse austenite. Fig. 12 b) presents the DL-EPR curve of specimen Q1-650 showing that, at this condition, with 7.5% of austenite, the activation and reactivation peaks can also be de-convoluted in two peaks. The splitting became more pronounced with the increase of austenite content (Fig. 12 a)), Q1-DT1), which confirms the findings of previous works [11,17].



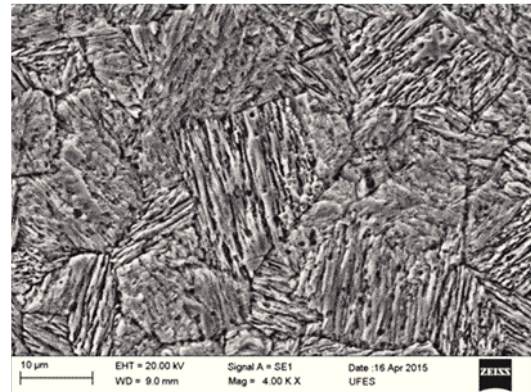
a)



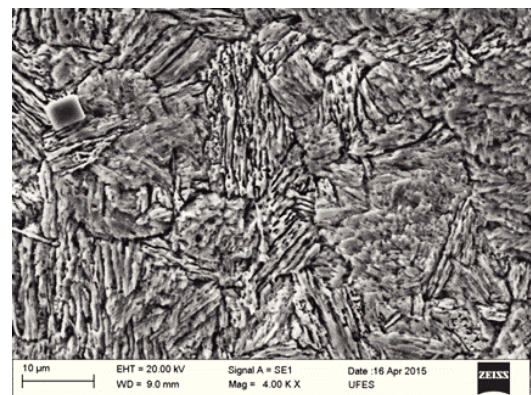
b)

Fig. 12. Examples of DL-EPR curves with splitting of activation and reactivation peaks: Q1-DT1 (a) and Q1-650 (b).

Figs. 13 a) and b) show the microstructures of specimens Q1-DT1 and Q2-DT1 after the DL-EPR tests. Interlath and intergranular attacks are clearly observed in double tempered specimens.



a)



b)

Fig. 13. Microstructures of specimens Q1-DT1 (a) and Q2-DT1 (b), after the DL-EPR tests.

#### 4. Conclusions

The sensitization of a Ti alloyed supermartensitic stainless steel was studied in this work using double loop electrochemical potentiodynamic tests and microstructural analysis. The main conclusions are:

- Specimen quenched from 1000°C (WQ-water quenched) showed the lowest degree of sensitization ( $I_r/I_a = A_r/A_a = 0.000$ ). Specimens double quenched (1000°C/WQ + 900°C/WQ) and triple quenched (1000°C/WQ + 900°C/WQ + 800°C/WQ) undergone increasing Ti(C, N) precipitation and, as a consequence, increasing degrees of sensitization (DOS). In these specimens, the corrosion attack was not restricted to grain boundaries;

- An increase of the degree of sensitization (DOS) was observed with the increase of tempering

temperature from 500°C to 600°C. For specimens single quenched (1000°C/WQ) and double quenched (1000°C/WQ + 900°C/WQ) the increase of tempering temperature to 650°C also caused a further increase of the DOS. Tempering at 650°C introduces reverse austenite in the microstructure, which forms between the martensite laths and in the previous austenite grain boundaries. Austenite is preferentially attacked due to its lower Cr and Mo contents;

– The specimen triple quenched (1000°C/WQ + 900°C/WQ + 800°C/WQ) and tempered at 650°C showed lower degree of sensitization (DOS) than single and double quenched steels tempered at the same temperature because its austenite content is lower;

– Sensitization could not be attributed to Cr carbides precipitation since these phases were not observed. Cr depletion around Ti(CN) particles is the most likely cause for sensitization of quenched specimens and quenched and low temperature (500°C and 600°C) tempered specimens. For specimens tempered at 650°C and double tempered (670°C/2h + 600°C/2h) the low Cr and Mo austenite formation also contributes to the sensitization process.

#### Acknowledgements

Authors acknowledge the Brazilian Research agencies CNPq and ANP for financial support.

#### References

- [1] C. Barbosa, I. Abud, *Recent Pat. Corros. Sci.* 3 (2013) 27.
- [2] F.G. Wilson, *Br. Corros. J.* 6 (1971) 100.
- [3] G.H. Aydoğdu, M.K. Aydinol, *Corros. Sci.* 48 (2006) 3565.
- [4] S. Frangini, A. Mignone, *Br. Corros. J.* 48 (1992) 715.
- [5] H. Nakamichi, K. Sato, Y. Miyata, M. Kimura, K. Masamura, *Br. Corros. J.* 50 (2008) 309.
- [6] A. Pardo, M.C. Merino, A.E. Coy, F. Viejo, M. Carboneras, R. Arrabal, *Acta Mater.* 55 (2007) 2239.
- [7] R. Leiva-García, J.C.S. Fernandes, M.J. Muñoz-Portero, J. García-Antón, *Corros. Sci.* 94 (2015) 327.
- [8] B. Guanshun, S. Lu, D. Li, Yiyi Li, *Br. Corros. J.* 90 (2015) 347.
- [9] E. Ladanova, J.K. Solberg, T. Rogne, *Corros. Eng., Sci. Technol.* 41 (2006) 143.
- [10] J.M. Aquino, C.A. Della Rovere, S.E. Kuri, *Corros. Sci.* 51 (2009) 2316.
- [11] C.A. Della Rovere, J.M. Aquino, C.R. Ribeiro, R. Silva, N.G. Alcântara, S.E. Kuri, *Mater. Des.* 65 (2015) 318.
- [12] G.F. da Silva, S.S.M. Tavares, J.M. Pardal, M.R. Silva, H.F.G. de Abreu, *J. Mater. Sci.* 46 (2011) 7737.
- [13] A.S. Lima, A.M. Nascimento, H.F.G. Abreu, P. de Lima-Neto, *J. Mater. Sci.* 40 (2005) 139.
- [14] J.K. Kim, Y.H. Kim, J.S. Lee, K.Y. Kim, *Corros. Sci.* 52 (2010) 1847.
- [15] T.M. Devine, A.M. Ritter, B.J. Drummond, *Metall. Trans. A* 12A (1981) 1981.
- [16] J.K. Kim, Y.H. Kim, B.H. Lee, K.Y. Kim, *Electrochim. Acta* 56(4) (2011) 1701.
- [17] V. Čihal, R. Štefēc, *Electrochim. Acta* 46 (2001) 3867.
- [18] B.D. Cullity, C.D. Graham, *Introduction to Magnetic Materials*, 2nd ed., Wiley and IEEE Press, USA, 2009.
- [19] C.A.D. Rodrigues, P.L.D. Lorenzo, A. Sokolowski, C.A. Barbosa, J.M.D.A. Rollo, *Mater. Sci. Eng., A* 460-461 (2007) 149.